Linköping University Pre-Print

Standard-free composition measurements of $Al_xIn_{1-x}N$ by low-loss electron energy loss spectroscopy

Justinas Palisaitis, Ching-Lien Hsiao, Muhammad Junaid, Mengyao Xie, Vanya Darakchieva, Jean-Francois Carlin, Nicolas Grandjean, Jens Birch, Lars Hultman and Per O.Å. Persson

This is the pre-peer reviewed version of the following article:

Justinas Palisaitis, Ching-Lien Hsiao, Muhammad Junaid, Mengyao Xie, Vanya Darakchieva, Jean-Francois Carlin, Nicolas Grandjean, Jens Birch, Lars Hultman and Per O.Å. Persson, Standard-free composition measurements of $Al_xIn_{1-x}N$ by low-loss electron energy loss spectroscopy, 2011, physica status solidi (RRL) – Rapid Research Letters, (5), 2, 50-52.
http://dx.doi.org/10.1002/pssr.201004407

Preprint available at: Linköping University Electronic Press
http://urn.kb.se/resolve?urn=urn:nbn:se:liu:diva-65816

Standard-free composition measurements of $Al_xIn_{1-x}N$ by low-loss electron energy loss spectroscopy

Justinas Palisaitis[*,1], Ching-Lien Hsiao[1], Muhammad Junaid[1], Mengyao Xie[1], Vanya Darakchieva[1], Jean-Francois Carlin[2], Nicolas Grandjean[2], Jens Birch[1], Lars Hultman[1] and Per O.Å. Persson[1]

[1] Department of Physics, Chemistry and Biology (IFM), Linköping University, SE-58183, Linköping, Sweden
[2] Ecole Polytechnique Fédérale de Lausanne (EPFL), CH 1015 Lausanne, Switzerland

Keywords: AlInN, low loss EELS, thin films, compositional analysis

* Corresponding author: juspa@ifm.liu.se

We demonstrate a standard-free method to retrieve compositional information in $Al_xIn_{1-x}N$ thin films by measuring the bulk plasmon energy (E_p), employing electron energy loss spectroscopy (EELS) in a scanning transmission electron microscope (STEM). Two series of samples were grown by magnetron sputter epitaxy (MSE) and metal organic vapor phase epitaxy (MOVPE), which together cover the full compositional range $0 \leq x \leq 1$. Complementary compositional measurements were obtained using Rutherford backscattering spectroscopy (RBS) and the lattice parameters were obtained by X-ray diffraction (XRD). It is shown that E_p follows a linear relation with respect to composition and lattice parameter between the alloying elements from AlN to InN allowing for straightforward compositional analysis.

Group III-nitride semiconductor alloy attracts interest due to promising applications for contemporary and future optoelectronic and electronic devices [1, 2]. For example, alloying the two binary nitrides InN and AlN results in the ternary compound $Al_xIn_{1-x}N$, with a bandgap that spans from 0.64 eV to 6.2 eV [2, 3]. $Al_xIn_{1-x}N$ is particularly attractive since it can be grown lattice matched to GaN and AlGaN [4], ensuring stress-free heterostructures with tunable bandgap [5]. Simultaneously, the constant size reductions of III–nitride device structures are accompanied by a need for increased control and understanding of growth and diffusion mechanisms [6, 7] along with accurate compositional and structural information.

RBS, elastic recoil detection analysis (ERDA), and secondary ion mass spectroscopy (SIMS) are commonly used for macroscopic compositional investigations. However, these methods are not adequate to investigate confined structures like quantum wells and dots, nor are they sufficient to investigate segregation to grain boundaries or single precipitates. Such spatial resolution is achieved by STEM where presently the resolution is below the atomic level [8, 9]. STEM is frequently combined with spectroscopy methods for compositional analyses such as energy dispersive X-ray spectroscopy (EDX) and EELS [10, 11]. However, EDX requires accurately known k-factors making such quantification difficult [12] and core-loss EELS require known scattering cross sections [13]. Furthermore, the EEL spectrum acquisition is often difficult due to low signal strength [14, 15]. However, the low-loss EEL spectrum exhibits the significantly stronger bulk plasmon peak which depends on the quasi free electron density that determines the local optical properties [16-18]. By employing a combination of low-loss EELS and STEM, it is thus possible to acquire a composition dependent measurement with significant spatial resolution. In this work we have measured the bulk plasmon energy, E_p, in $Al_xIn_{1-x}N$ structures throughout the full range of x ($0 \leq x \leq 1$). Compositional measurements were also obtained from the same structures using RBS and the lattice constants were obtained by XRD.

Two series of epitaxial single layer $Al_xIn_{1-x}N$ samples, A and B, were grown using ultra-high vacuum MSE [19] and MOVPE [20], respectively. The A-series samples ($0 \leq x < 1$) were grown at room temperature with a total thickness of ~100 nm on top of an AlN seed layer grown at 1000 ^oC on $Al_2O_3(0001)$. The A-series AlN film (x=1 ~200

nm) was grown at 1000 °C on Al_2O_3(0001) [21]. The B-series with compositional range $0.78 \leq x \leq 0.88$ were grown at 820 °C, resulting in ~100-120 nm thick films on top of a 1 µm-thick GaN buffer layer on Al_2O_3(0001) [20]. The two series of samples cover the full compositional range $0 \leq x \leq 1$ and partly overlap.

θ-2θ measurements were obtained from the as-grown samples using a Philips X'pert diffractometer. Compositional measurements by RBS were obtained using a 2 MeV He+ beam with an incidence angle of 7° off from the surface normal and back scattered ions were detected at an angle of 172°. The experimental data were simulated by SIMNAR 6.03 software [22].

All (S)TEM and EELS analyses were performed using an Tecnai G^2 TF 20 UT (S)TEM, employing a Gatan ENFINA parallel EEL spectrometer. The low-loss spectra were recorded in image-coupled mode using a <1nm electron probe, 1 mm spectrometer entrance aperture. Gatan DigitalMicrograph was employed to determine E_p by averaging 500 spectra. Low-loss EEL spectra for each $Al_xIn_{1-x}N$ structure were obtained by initial zero loss peak fitting, followed by Fourier-log deconvolution [11] for plural scattering removal and finally fitting the E_p using non-linear least squares fitting (NLLS) in the central part of the plasmon peak.

The A-series samples cover the full compositional range from InN to AlN, while the B-series samples are all Al rich such that $x_{min}=0.78$. The sample notation identifies the series (A or B) and associated Al concentration, e.g. MSE grown $Al_{0.28}In_{0.72}N$ is denoted by A0.28. The samples which were investigated in this study are presented in Table I, showing the corresponding compositional information from RBS, the respective lattice parameters measured by XRD and the E_p as obtained with EELS.

Table 1 Summary of studied samples containing composition obtained by RBS, lattice parameters *a* and *c* by XRD and bulk plasmon energy, E_p, by low-loss EELS are given in the table.

Sample	RBS, at. %			XRD, Å			E_p, eV
name	Al	In	N	*c*	*a*	*c/a*	
A0.00	0	49	51	5.73	3.58	1.59	14.95
A0.28	14	36	50	5.55	3.45	1.60	16.11
A0.44	22	28	50	5.40	3.35	1.61	17.25
A0.66	33	17	50	5.25	3.27	1.60	18.62
A0.84	42	8	50	5.11	3.19	1.59	19.64
A1.00	49	0	51	4.98	3.11	1.60	20.46
B0.78	39	11	50	5.14	3.18	1.61	19.30
B0.84	42	8	50	5.09	3.18	1.60	19.64
B0.88	44	6	50	5.05	3.17	1.59	19.69

Figure 1 a)-f) show the TEM investigations from the A-series $Al_xIn_{1-x}N$ single layers. As can be seen, the layers exhibit a relatively smooth surface. The layers have a high point defect density, owing to the low sputtering temperature, and are all ~100 nm thick. The AlN buffer layers and Al_2O_3 substrates can also be seen, and the interfaces are indicated by arrows. Diffraction patterns obtained along the [11-20] zone axis reveal the changing position of the $Al_xIn_{1-x}N$ (0002), (1-100) and (1-102) reflections (higher orders not shown), corresponding to the different *a* and *c* lattice parameters, respectively, following the compositional differences and associated lattice parameter. The observed variations are in agreement with the lattice parameter change obtained by XRD.

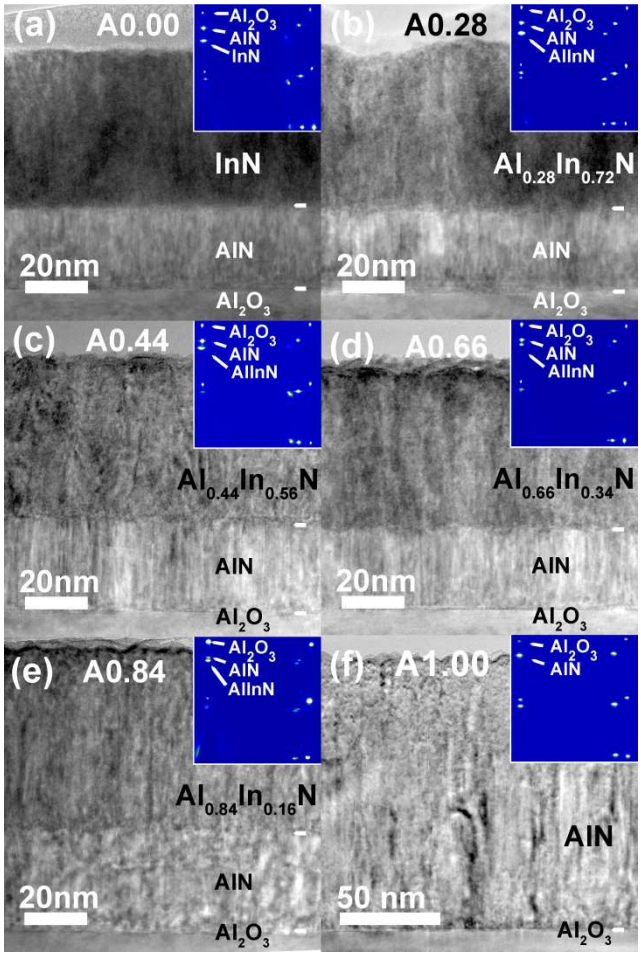

Figure 1 (a)-(f) Cross-sectional TEM images showing the A-series of the $Al_xIn_{1-x}N$ samples grown on AlN buffer layer and Al_2O_3 substrate and corresponding selective area diffraction pattern for each sample along [11-20].

The low-loss EEL spectra for all investigated samples from A0.00 to A1.00, including the B-series, are presented in figure 2. As can be seen, the energy loss of the bulk plasmon peak increases continuously from 14.95 eV (InN) to 20.46 eV (AlN). These values deviate slightly from reported values for InN=15.5 eV [23] and AlN=21.2 eV [24] and may be due to different peak fitting procedures.

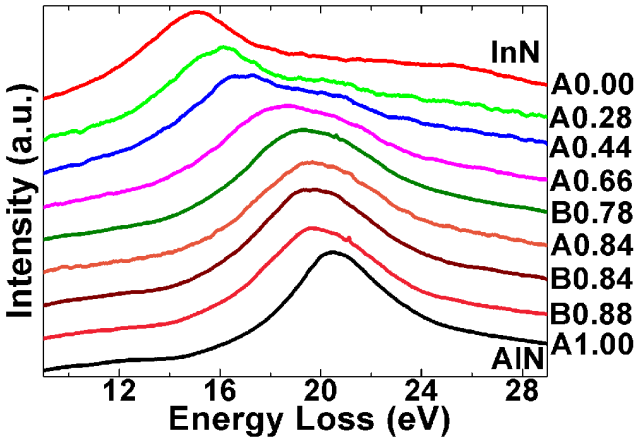

Figure 2 Low-loss EEL spectra showing the shift in plasmon energy (E_p) of the A and B $Al_xIn_{1-x}N$ samples in compositional order from InN (top spectrum, x=0) to AlN (bottom spectrum, x=1).

A shoulder feature is present in some spectra at about 20 eV, corresponding to the position of the pure AlN plasmon peak. This may indicate AlN phase separation in the material. However, the contribution of this shoulder to the final spectrum is about 1% of the total intensity. Assuming identical scattering cross sections of the bulk plasmon throughout the alloying range, any phase separation of AlN does not change the overall composition significantly.

The variation in E_p with respect to composition and *c*-lattice parameter is shown in Figure 3. As can be seen, E_p increases linearly with respect to both composition and lattice parameter following a relation determined from a linear fit to the experimental data:

$$E_p(Al_xIn_{1-x}N)=5.69x+14.78 \qquad (0\le x\le 1) \qquad (1)$$

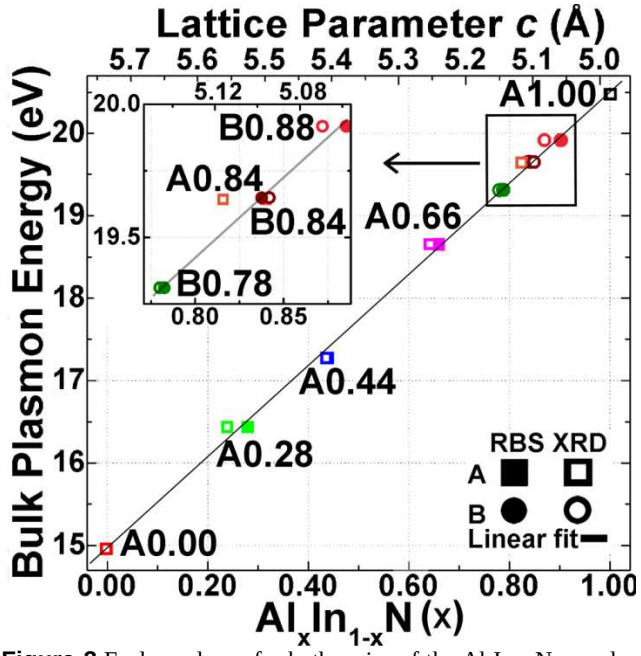

Figure 3 E_p dependence for both series of the $Al_xIn_{1-x}N$ samples as a function of composition and lattice parameter c.

E_p is related to the free carrier density in the material where the plasmon is excited and depends on structure and lattice parameter, which may be strained. In this investigation, all studied $Al_xIn_{1-x}N$ layers of a continuous wurtzite structure were isotopically strained by ~0.5%. This strain is not expected to contribute significantly to the result, as has been demonstrated on strained AlN layers (not shown here). The electron momentum transfer (q) also affects the measured E_p [10], by applying identical experimental conditions, the observed shift is interpreted as a direct change in sample composition. The E_p in the overlapping range between the A and B series agree very well (fig. 3), which demonstrate that this method is independent of growth technique and nucleation scheme used. Slight deviations from the linear fit are observed in figure 3, which may be explained by minor errors in the experimental methods applied here, compositional fluctuations due to phase separation, the presence of strain in layers, and a small deviation from Vegard's rule for the lattice parameters [20].

In conclusion, we have demonstrated that low-loss EELS is a powerful method for compositional determination in $Al_xIn_{1-x}N$, as the plasmon energy of this system varies linearly with *x*. This provides a fast, simple, and standard-free method for assessing the alloy composition. It is suggested that the method is applicable with a spatial resolution in the nanometer range and that this method can be expanded to related systems, such as InGaN and AlGaN, and other semiconductor alloys.

References

[1] S. Strite et al., J. Vac. Sci. Technol. B **10**, 1237 (1992).
[2] J. Wu, J. Appl. Phys. **106**, 011101 (2009).
[3] C. L. Hsiao et al., Appl. Phys. Lett., **91**, 181912 (2007).
[4] R. Butte, et al., J. Phys. D: Appl. Phys. **40**, 6328 (2007).
[5] I. Vurgaftman et al., J. Appl. Phys. **89**, 5815 (2001).
[6] S. Nakamura et al., Appl. Phys. Lett. **67**, 1868 (1995).
[7] S. Senda et al., Appl. Phys. Lett. **92**, 203507 (2008).
[8] K. Kimoto et al., Micron **39**, 257 (2008).
[9] E. M. James et al., Ultramicroscopy **78**, 125 (1999).
[10] D. B. William and C. B. Carter, Transmission Electron Microscopy: A Text Book of Materials Science (Plenum, New York, 1996), Vols. 1–4.
[11] R. F. Egerton, Electron Energy-Loss Spectroscopy in the Electron Microscope (Plenum, New York 1996).
[12] M. Malac et al., Microsc Microanal **5**, 29-38 (1999).
[13] F. Hofer, Microsc. Microanal. Microstruc. **2**, 215, (1991).
[14] M. Bosman et al., Ultramicroscopy **108**, 837 (2008).
[15] K. Leifer, et al., Micron **311**, 411–427 (2000).
[16] A. Howie, Micron, **34**, 121 (2003).
[17] M.Stoger-Pollach et al., Ultramicroscopy **108**, 439 (2008).
[18] W. Sigle et al., Ultramicroscopy **96,** 565 (2003).
[19] T. Seppänen et al., J. Appl. Phys., **97**, 083503 (2005).
[20] V. Darakchieva et al., J. Appl. Phys. **103**, 103513 (2008).
[21] C.-L. Hsiao, et al.,… (2010).
[22] www.rzg.mpg.de/~mam/
[23] K.A. Mkhoyan et al., Appl. Phys. Lett. **82**, 1407 (2003).
[24] M. Benaissa et al., Appl. Phys. Lett. **95**, 141901 (2009).